Simulative design method for decentral air handling unit including air-to-air heat pump

Tobias Fröhlingsdorf[1]*, *Martin* Kremer[1], and *Dirk* Müller[1]

[1]Institute for Energy Efficient Buildings and Indoor Climate, RWTH Aachen University, Germany

Abstract. Since people spend around 90 % of their daytime in buildings, the energy demand in buildings to maintain thermal comfort is remarkable. By developing a decentralized air handling unit (AHU), equipped with a R290 heat pump, it is targeted to reduce the installation time in buildings and the CO_2 emissions for air conditioning. To integrate decentralized AHU with heat pumps in residential or non-residential buildings, these must be carefully designed in advance to get the highest efficiency. The development process considers a wide range of aspects, including energy demand, component design and acoustics. The simulation results in a total heating load of 1080 W. The load is distributed in 500 W of the sensible heat in the energy recovery system, 500 W through the condenser of the heat pump and 80 W through the electric air pre-heater for frost protection. After design and component selection, the decentralized AHU was built up as a demonstrator. The comparison of simulation and experiments prove the validity of virtual pre-development by showing a maximum deviation of 5 % in the heat flow of all components in heating mode by using constant efficiency models.

1 Introduction

Global warming challenges several industries and companies are trying to reduce CO_2 emissions above all areas of product development [1, 2]. Buildings accounts for a large share of CO_2 emissions which offers high potential for energy reduction [3]. Lowering CO_2 emissions while maintaining thermal comfort in buildings is the main target. Governments in Europe decided on renovation standards for buildings to reduce heat losses. But increased isolation of buildings requires mechanical ventilation to prevent moulding [4, 5]. Decentral ventilation used in modern building standards is one of the measures to maintain thermal and hygienic comfort in rooms. Heat exchangers in an AHU need an external heat source or sink for heating and cooling the air. Typically, water-based heat exchangers are used inside the AHU. Those heat exchangers are cross-flowed by a conditioned glycol-water and air mass flow. Since these heat exchangers need hoses and tubes for an energy supply, a high effort in renovation is needed to integrate decentral ventilation. Therefore, this paper presents a pre-design method for a decentral monobloc AHU with an integrated energy recovery system and a heat pump. The heat pump transfers heat from the extracted room air to the supply air and requires only electrical energy providence. Sockets are already well provided in any type of building. In addition, the small-sized compressor of the heat pump requires low electrical power outputs which do not overload the electrical cables in the building. This paper is aiming to present multiple possible topologies for a decentral AHU and recommendations for parameters used in simulation models for the evaluation of decentral AHU with an integrated heat pump.

2 Selection of AHU topologies

While designing a decentral AHU with an energy recovery system (ERS) and a heat pump, there are several possibilities for positioning heat exchangers (HX) in the airflow. In Table 1 is given an overview of all investigated topologies and highlighted their differences in equipment.

Table 1. Overview of all investigated topologies.

Topology	1	2	3	4	5	6	7	8	9
EHA HX	X	X	X	X	X	X	-	-	-
ETA HX	X	X	X	-	-	-	X	X	X
ERS	-	-	-	X	X	X	X	X	X
SUP Bypass	-	X	X	-	X	X	-	X	X
EHA Bypass	-	-	X	-	-	X	-	-	X

When positioning a heat exchanger of the heat pump in the exhaust air channel (EHA), there is an “X” in the topology column. Same principle works for a heat exchanger in the extract air channel (ETA). Since

* Corresponding author: tobias.froehlingsdorf@eonerc.rwth-aachen.de

topology #1 to #3 are not equipped with an ERS, the EHA HX is the same as the ETA HX and therefore, crosses ("X") are in both columns. In the topologies #4 to #9, additionally a membrane-based enthalpy exchanger as ERS is considered. To increase energy efficiency and heating capacity, the option of secondary air with a bypass from extract to supply air (SUP bypass) as well as a bypass from outdoor air to exhaust air (EHA bypass) is included. Fans will be positioned right before the duct output. In topologies with an ERS, the supply air fan is positioned before the ERS due to better acoustical performance.

All introduced topologies from Table 1 are presented in Figure 1 to Figure 3. The bypass to supply air (#2, #3, #5, #6, #8 and #9) is formatted as a dashed line and the bypass to exhaust air (#3, #6, #9) as a dot-dashed line.

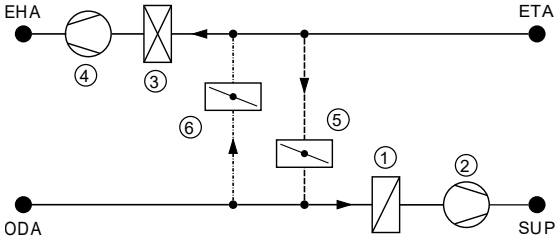

Fig. 1. Decentral AHU topology for #1 to #3.

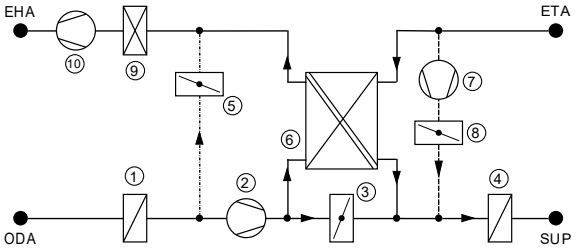

Fig. 2. Decentral AHU topology for #4 to #6.

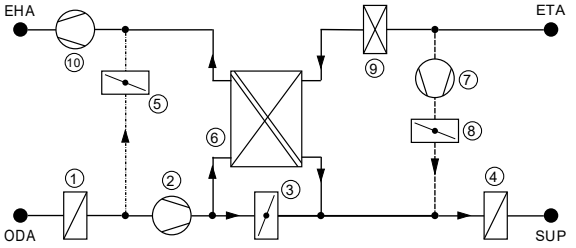

Fig. 3. Decentral AHU topology for #7 to #9.

The topologies #1 to #3, which are shown in Figure 1, are not equipped with an ERS. Both fans {(2), (4)} are positioned at the outlet of each air channel and the heat exchangers of the heat pump are immediately in front of the fans {(1), (3)}. Integrated flaps in the supply air bypass (5) and in the exhaust air bypass (6) are open at demand.

The topologies in Figure 2 integrates an ERS (6) and uses the EHA heat exchanger (9). Both fans {(2), (10)} are positioned on the outer side of the ERS. The supply bypass requires an additional fan (7) due to the supply air fan position upstream of the ERS. The airflow in the SUP bypass and ERS flows through the SUP heat exchanger (4). An additional bypass for the ERS (3) is used if the AHU operates in cooling mode.

All topologies with an ETA heat exchanger are shown in Figure 3. Except for the switched position of the heat exchanger (9), the topologies in Figure 2 and Figure 3 are identical.

3 Evaluation of AHU topologies

Simulation models of all topologies are created for simulative evaluation according to the required energy demand. Modelica (version 3.2.3) is used as modelling language. All simulations are carried out in the simulation software Dymola 2021. Furthermore, building models are set up with standard components from the open-source library AixLib [6].

The topology with the lowest energy demand is transferred to a demonstrator and investigated experimentally to proove the reliability of the simulation model.

3.1 Simulation methodology

Simulations are used to determine the electrical and thermal energy demand of the decentral AHU. In this study of topologies, constant parameters for the efficiencies of the ERS and heat pump model will be used to compare all topologies. Afterwards the component requirements need to be derived for building a demonstrator of the AHU.

Each simulation is executed by using specified data sets for the user profile, weather data and the building parameters. The validated models for the three parts of the environment are taken from the AixLib [6]. In this case, the infrastructure of the façade test bench is reproduced. Therefore, the occupant behaviour profile is chosen as a two-person office from SIA 2024 and considers a total hygienic airflow $\dot{V}_{\mathrm{hyg}}$ of 72 $m^3 \cdot h^{-1}$ [7, 8]. The room in the used façade test bench has an area of 24 m^2 and a volume of 65 m^3. For the validation of the simulation results, the AHU will be designed especially for the façade test bench and the use case of the two-person office. The façade test bench is built for this use case and considers internal heat- and CO_2 sources for reproducing occupant behaviour. Although different measures are done, the infiltration rate of the façade test bench is with 0.2 h^{-1} higher than in modern standards. The simulations using a constant infiltration rate. In the weather model is a test reference year data set for Aachen (Germany) used. The building parameters are used from the façade test bench. For concept studies, the approach of a reduced-order model is chosen [9]. The temperature of the room air volume is homogenous distributed. All surrounding wall elements (inner wall, outer wall, ceiling and floor) are modelled as with a thermal capacity and resistance. Except the outer wall, all elements are adiabatic since the temperature on the outside of the wall is permanently set to 20 °C.

The model for the AHU represents the topology and components inside. The integrated fans, flaps and heat exchangers are parameterized depending on the AHU topology. As an example, the nominal mass flow of the EHA fan is higher in a topology with an EHA bypass

than in a system without. The ERS inside the AHU is parameterized by a constant efficiency for sensible and latent heat exchange. For the energy demand simulations of all topologies, the sensible efficiency is set to 75 % and the latent efficiency is set to 60 % [10]. The heat pump is based on calculations for the carnot COP multiplied with an overall energy conversion efficiency of 35 % [11, 12]. Both models of ERS and heat pump are used and validated in previous projects [6].

On top of the AHU is a control model which applies operation strategies. If available, the control model opens or closes the flaps, set the compressor load of the heat pump and the air volume flow from all fans. At night (between 10 pm and 6 am) the control model sets $\dot{V}_{hyg}$ to 20 $m^3 \cdot h^{-1}$ for the reduction of the energy demand. The air volume flow through the heat exchanger of the heat pump is increased due to the bypass up to a total of 144 $m^3 \cdot h^{-1}$ depending on the compressor load. In night mode, the compressor load is limited to 30 % of the nominal electrical compressor power $P_{el,HP}$ of 200 W. The heating mode is turned on if the room temperature T_{Room} is below 20 °C (± 1 K). If T_{Room} rises above 26 °C (± 1 K), cooling mode is activated. Additionally, the ERS bypass is closed if T_{Room} is below 21 °C or lower than the outdoor air temperature T_{ODA}, when the AHU is in cooling mode. The control model maintains T_{Room} in the range of 20 °C to 26 °C [13]. For reasons of frost protection in the ERS, the electrical pre-heater will heat T_{ODA} to -5 °C.

3.2 Simulation results

Dynamic simulations are executed for 365 days. The room temperature T_{Room} is shown in Figure 4. The temperature is displayed in descending order. One can see that T_{Room} is for three months higher than 21.3 °C or T_{Room} is for twelve months higher than 16 °C in all shown topologies. Since the temperature profile of the topologies #1, #2 and #3 hardly differ, one curve is selected as an example for illustration. Same procedure was applied for topologies #4, #5 and #6 as well as #7, #8 and #9. The curve starts at maximum room temperatures of 27 °C. In this period the AHU is working in cooling mode since we are above 26 °C. Then it decreases to 26 °C and the gradient lowers until 20 °C is reached. The topologies with ERS are showing a plateau at 21 °C before reaching 20 °C. Then 20 °C will be hold a long time, until the temperature drops to the lowest T_{Room} of 16 °C due to night mode.

In Figure 5 is the supply air temperature T_{SUP} shown. The visualization of the curves is also in descending order and only one curve shown for each kind of heat exchanger position in the topologies. The curve starts at maximum temperatures from 34 °C for peak loads in the year. Then it decreases in topology #3 constantly to 13 °C and has a lower peak at 6 °C. The topologies #6 and #9 aren't showing that constantly behaviour, instead there are some variations in the gradient until the temperature of 18 °C is reached. A lower peak at 12 °C in both topologies are recognizable.

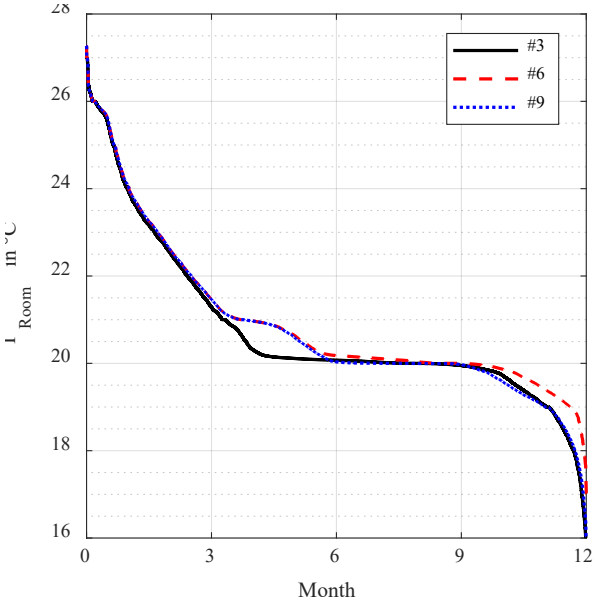

Fig. 4. Descending sorted room temperatures for topology #3, #6 and #9.

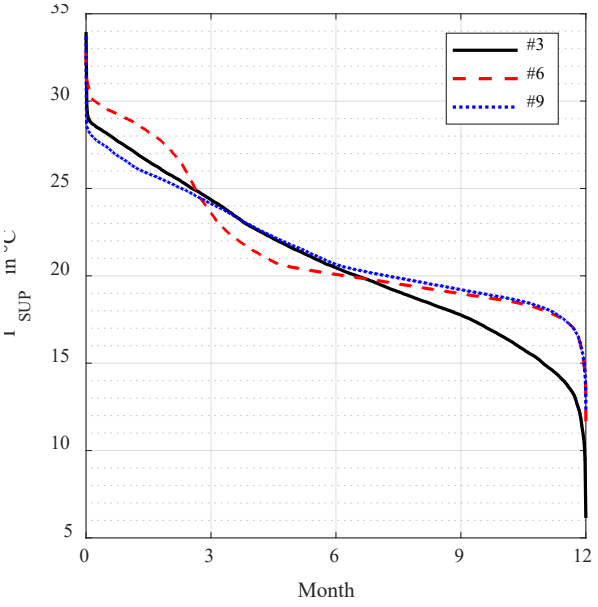

Fig. 5. Descending sorted supply air temperatures for topology #3, #6 and #9.

In the next step the cumulated heat energy demand Q_{total} of all components is displayed in Figure 6. Each topology is displayed in a single bar, labelled on the x-axis. Each bar is divided in the share of the ERS, electric pre-heater (E-Heater), heat pump in heating mode (HP heat) and the heat pump in cooling mode (HP cool).

In the last step the cumulated electrical energy demand $W_{el,total}$ of all components is displayed in Figure 7. The electrical energy demand is the necessary amount of energy to be supplied from outside the AHU. Since the ERS does not need any electrical energy, the bar is divided in the share of E-Heater, the heat pump and all fans.

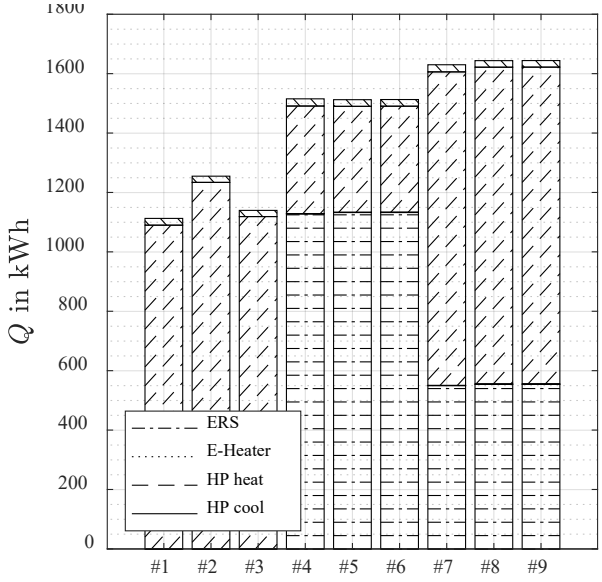

Fig. 6. Thermal energy demand of all topologies.

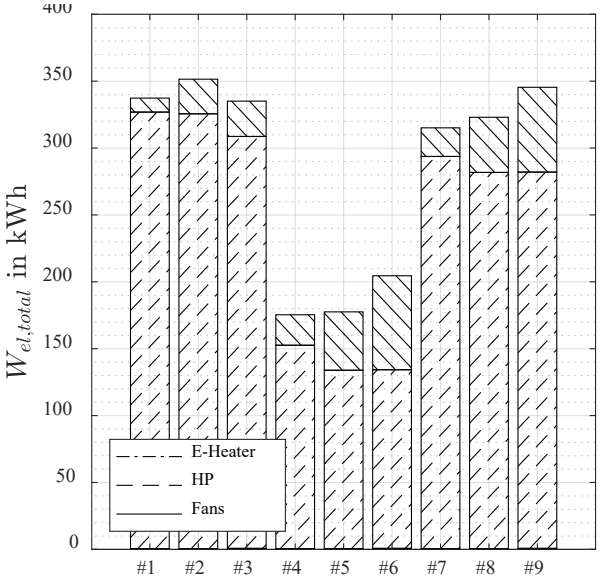

Fig. 7. Electrical energy demand of all topologies.

3.3 Discussion

The curve of T_{Room} in Figure 4 compares the topologies in maintaining thermal comfort criteria. It is recognizable if and how often T_{Room} is outside the boundaries of 20 °C to 26 °C. At start of the curve the temperatures are above 26 °C and the AHU is in cooling mode. In cooling mode is the ERS bypassed. That means, that the extract and supply air flows in all topologies with the same temperature into the heat exchangers of the heat pump. For all topologies are in this case no differences in cooling mode and therefore the lines lie on top of each other above 26 °C. The curves start deviate after three months and a temperature of 21.5 °C. The gradient for topologies #6 and #9, with integrated ERS, is lowering until a plateau on 21 °C is reached. This is due to the ERS bypass control which opens at 21 °C. Topology #3 falls constantly down to 20 °C until a plateau is reached. In the months 9 to 12 is T_{Room} falling below 20 °C due to the hysteresis controller of the room temperature, which is working between 21 °C and 19 °C. Furthermore, the gradient at 19 °C increases and lower peaks until 16 °C can be seen in Figure 4. Those lower peaks represent cold winter nights when the compressor power of the heat pump is limited, and not enough heat flow is available. In topology #6 is the supply air pre-heated in the ERS. T_{Room} sinks less due to the use of the ERS.

In Figure 5 is T_{SUP} displayed due to prove that thermal comfort criteria are maintained, as T_{SUP} is below the maximum temperature limit of 52 °C [4]. Even if it is not visible when the heat pump is active in Figure 5, it is mentionable that T_{SUP} has an influence on the condensation (heating mode) and evaporation (cooling mode) temperature of the refrigerant in the heat pump. According to the carnot model, the greater the temperature difference between condensation and evaporation, the lower is the coefficient of performance (COP). The control model is not controlling T_{SUP} and conditioning the supply air to comfortable temperatures. An additional heat flow is required to prevent a T_{SUP} below a comfortable temperature of e.g., 15 °C. The lowest T_{SUP} shows up when T_{Room} is above 20 °C at low outside temperatures.

The evaluation of topologies starts with the cumulated heat energy demand in Figure 6. The share of the E-Heater is for all topologies without EHA bypass at 0.52 kWh and with EHA bypass at 0.78 kWh. Due to the small shares for the E-Heater, the energy share is not visible in Figure 6. Since T_{Room} was similar for all topologies above 26 °C, the energy share for cooling (HP cool) equals also for all topologies. Due to the infiltration rate of the façade test bench, the heating mode dominates in the energy share. Since topology #1 to #3 does not include an ERS, all heat energy for heating and cooling is generated by the heat pump. The main difference of positioning the heat exchanger of the heat pump in ETA or EHA is visible in the energy share of the ERS in topologies #4 to #9. While having a higher

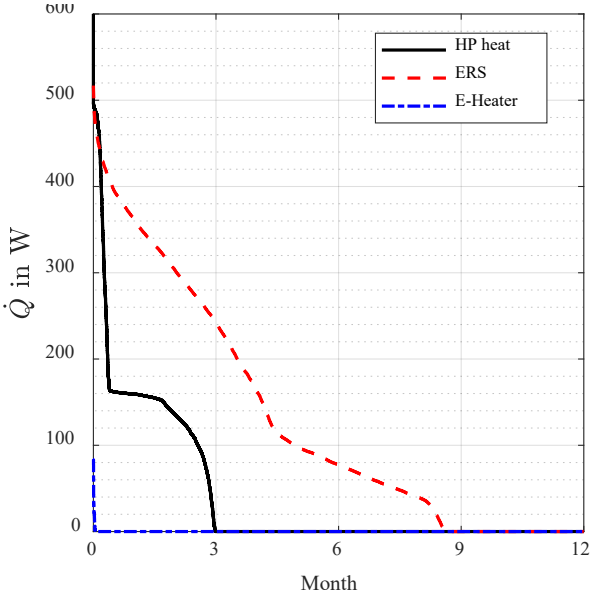

Fig. 8. Thermal energy demand according to topology #6 for each component.

inlet temperature difference in the ERS for topologies #4 to #6, the transferred heat energy is almost doubled compared to #7 to #9. The energy share for heating over the heat pump is in topology #4 to #6 less than in #7 to #9.

The cumulated electrical energy demand of all topologies is compared in Figure 7. The E-Heater is due to the small share of thermal energy and an assumed efficiency of 95 % not visible in Figure 7. The major share of the electrical energy accounts to the heat pump. Topologies #4 to #6 are showing the lowest share of electrical energy. The annual COP for the topologies #1 to #3 varies between 3.5 and 4.2, for the topologies #4 to #6 between 2.4 and 2.8 and for the topologies #7 to #9 between 3.9 and 4.1. The higher difference of entrance temperatures at the heat exchanger in topology #4 to #6 leads to a decreased COP. Despite this, the ERS is capable to reduce the required heat energy from the heat pump that the topologies #4 to #6 seems to be the topologies with lowest electrical energy demand.

With reference to the electrical energy demand of all topologies, it is recommended to position the heat exchangers of a heat pump for decentral AHU in SUP and EHA channel. Since the control model is simplified, the difference between the topologies can be varied by e.g. more efficient control of the supply air bypass. In that case, secondary air over the SUP bypass will mixed with the supply air to increase T_{SUP}. This reduces the heat losses in the room and reduces the operating time of the heat pump.

Finally, the total electrical energy demand of all topologies is lowest in the topologies #4 to #6. The demonstrator is built with an integrated ERS and the heat exchanger in the exhaust air channel. Because the flaps can be optionally opened, the demonstrator will be built as #6 with the option to operate as #4. Additionally, the control model will be optimized to reduce ventilation energy demand and increase the use of thermal energy in secondary air over SUP bypass.

3.4 Derive component requirements

Before building an AHU, the simulation results from topology #6 need to be analysed for selection of fans, refrigerant compressor and heat exchangers. The component requirements will be derived from the simulations of the façade test bench with an infiltration rate from 0.2 h^{-1}.

The descending heat flow for heating of the heat pump is displayed in Figure 8. The AHU is primarily designed for the heating mode and therefore, provide anytime a T_{Room} of 20 °C. In cooling mode, the maximum available power applies but the upper limit of T_{Room} at 26 °C can be exceeded. The compressor must be able to generate the heating power under consideration of the used refrigerant. The demonstrator is equipped with an R290 compressor, since R290 has a low global warming potential (GWP), high SCOP for building applications and currently wide offer on the market [14]. After designing all refrigerant pipes in CAD, the calculated refrigerant mass after [15] leads to 138 g that is below the legal limit of 150 g in Germany [16].

The ERS should also provide a maximum heat flow of 500 W for the hygienic air volume flow of 72 $m^3 \cdot h^{-1}$. The electrical heater for frost prevention of the ERS heats the incoming air flow and needs a heating power of at least 80 W for minimal outdoor air temperatures of -10 °C in Aachen. The lowest outdoor air temperatures occur at night where the AHU is in night mode with reduced air volume flow.

As described in section 3.1, the fans of the demonstrator are designed for at least 144 $m^3 \cdot h^{-1}$ to satisfy hygienic and thermal requirements. After component selection, pressure losses in the air channel are derived from CAD model. At least, radial fans are chosen for an operating point of 72 $m^3 \cdot h^{-1}$ providing a pressure increase of 300 Pa.

4 Validation of simulation method

For the validation of the derived component requirements, the demonstrator is operated in stationary working points for heating and cooling. The first working point represents the AHU in heating mode with an outdorr temperature at the inlet of the ERS $T_{ODA,ERS,in}$ of 5 °C and an inlet temperature in the extract air at the ERS $T_{ETA,ERS,in}$ of 19 °C. In the second working point, the AHU is operating in cooling mode with an outdoor temperature at the inlet of the heat exchanger of the heat pump $T_{SUP,HP,in}$ of 19 °C and an inlet temperature in the exhaust air at the heat exchanger of the heat pump $T_{EHA,HP,in}$ of 30 °C. Simulations and measurements are executed with a constant air volume flow of 72 $m^3 \cdot h^{-1}$.

For a reliable simulative pre-design, it is mandatory that the efficiencies of the ERS and heat pump model in chapter 3.1 are well chosen. The simulation model was parameterized due to a pre-study of available data sheets of relevant components.

4.1 Results

By comparing the temperatures at inlet and outlet of the ERS and both heat exchangers of the heat pump, as well as the heat flow inside the component, the results will prove the assumed efficiencies in the simulation model. All measured temperatures (four PT100 sensors across HX area) are averaged over the heat exchanger area. The heat flow is calculated using the measured air volume flow.

In the working point for heating, the temperatures at the ERS are shown in Figure 9. Since $T_{ODA,ERS,in}$ and $T_{ETA,ERS,in}$ are used in simulation extracted from measurement, the signals are identical. The dynamic behaviour is similar between measurement and simulation data. The comparison of the supply air heat flow in the ERS in measurement and simulation is displayed in Figure 10. The temperatures in the condenser and evaporator of the heat pump are compared in Figure 11. In this case the heat flow at the condenser in supply air is shown in Figure 12.

In the cooling mode the inlet and outlet temperatures at both heat exchanger is shown in Figure 13. The simulation inherits the inlet temperatures from the measurement data. Furthermore, the heat flow at the

evaporator is shown in Figure 14. In the case of cooling, the initialization in the simulation model shows a deviation in the temperatures.

4.2 Discussion

While heating the supply air in the AHU, the temperatures at the ERS and both heat exchanger of the heat pump showing similar dynamic behaviour. The $T_{SUP,ERS,out}$ differs in an average of 0.8 K between measurement and simulation. The sensible efficiency in measurement is calculated to 72 % compared to 75 % in simulation, which explains the slightly lower outlet temperature. But the measured temperature $T_{EHA,ERS,out}$ is also below the temperature in simulation. Since the temperature sensors are placed immediately at the outlet, heat losses are not expected. The average difference of the upper row temperature sensors compared to the lower row is 2 K. The same effect is detected at the exhaust air outlet. The average temperature decreases the temperature profile and increases the deviation between measurement and simulation.

With consideration of the deviations in the temperature, the heat flow in the ERS can differ for 5 % at the maximum in minute 15. By regarding the discussed uncertainites, the ERS predicts sufficient the behavior in the demonstrator.

Since the heat exchanger of the heat pump are positioned right behind the ERS, the inlet temperatures in Figure 11 should be equal to the outlet temperatures of Figure 9, but minor differences are visible in the exhaust air. Due to an increased temperature in measurement, heat is absorbed in the air duct from the environment of 19 °C. The supply air in simulation shows a constant offset of 2 K compared to the measured data. By having the identical air volume flow, the heat flow must be higher which is shown in Figure 12. The thermal inertia of the heat exchangers is not well modelled since the temperature drops immediately after turning off the heat pump. This lacks in evaluation of the demonstrator at dynamic behavior, but for comparison of stationary working points the dynamic behavior of the simulation model is neglected.

In the case of cooling, the temperatures in Figure 13 deviate more than in the heating mode, especially for the outlet temperature at the condenser in the exhaust air. Despite that, the dynamic of the heat flow in Figure 14 shows the same behaviour as the outlet temperature from the evaporator in supply air. Due to the lower supply air temperature in measurement, the heat flow for cooling is increased. The simulation model shows deviation in cooling power, which leads to a higher supply air temperature. Since the heat pump is in the demonstrator designed for the heating mode, the efficiency of the heat exchangers in cooling is decreased. By reversing the refrigerant flow, the air flow has in the first tube row the highest possible temperature difference. For this case, the carnot efficiency should be validated which is not possible for pre-studies. Hence, it is recommended for the built demonstrator to focus only on the heating mode.

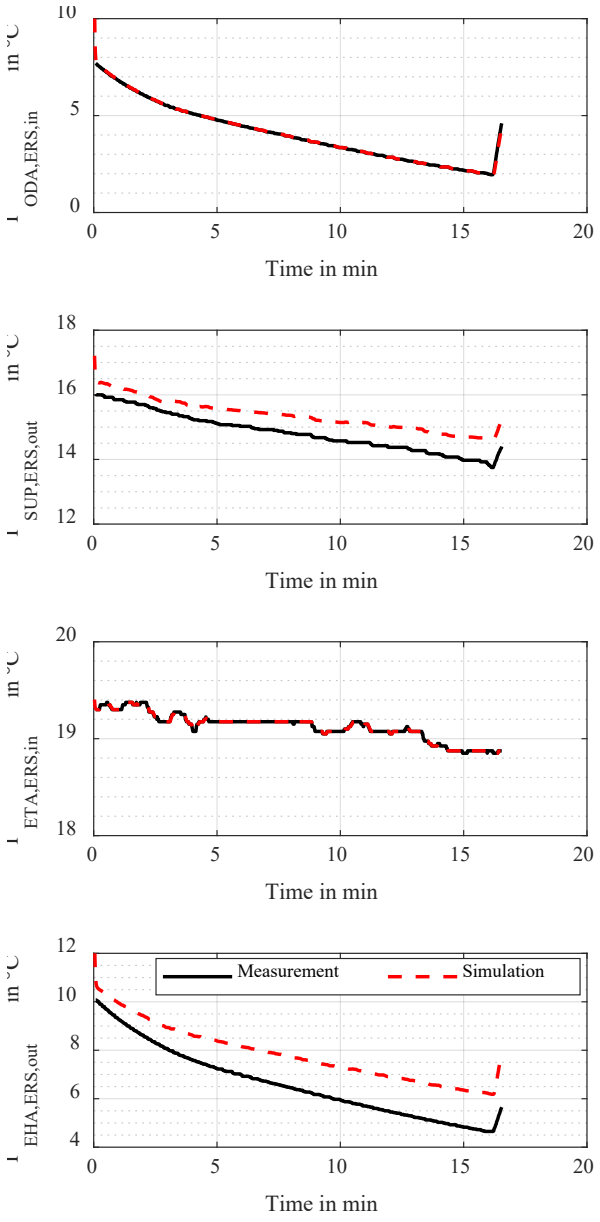

Fig. 9. Temperature comparison at ERS in heating mode.

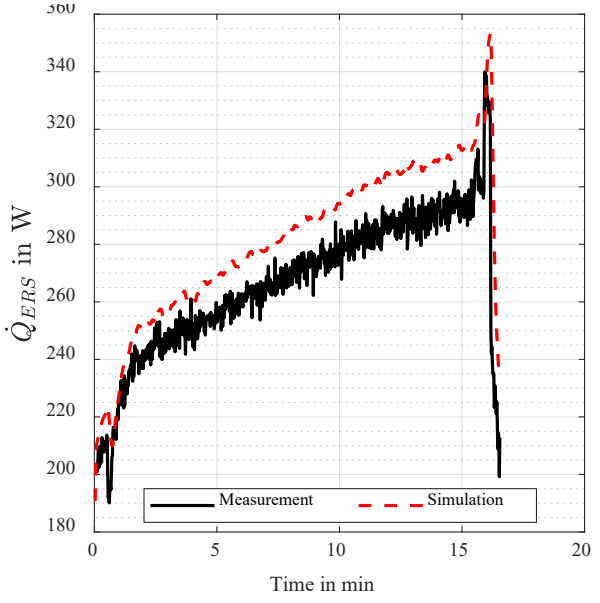

Fig. 10. Heat flow comparison at ERS in heating mode.

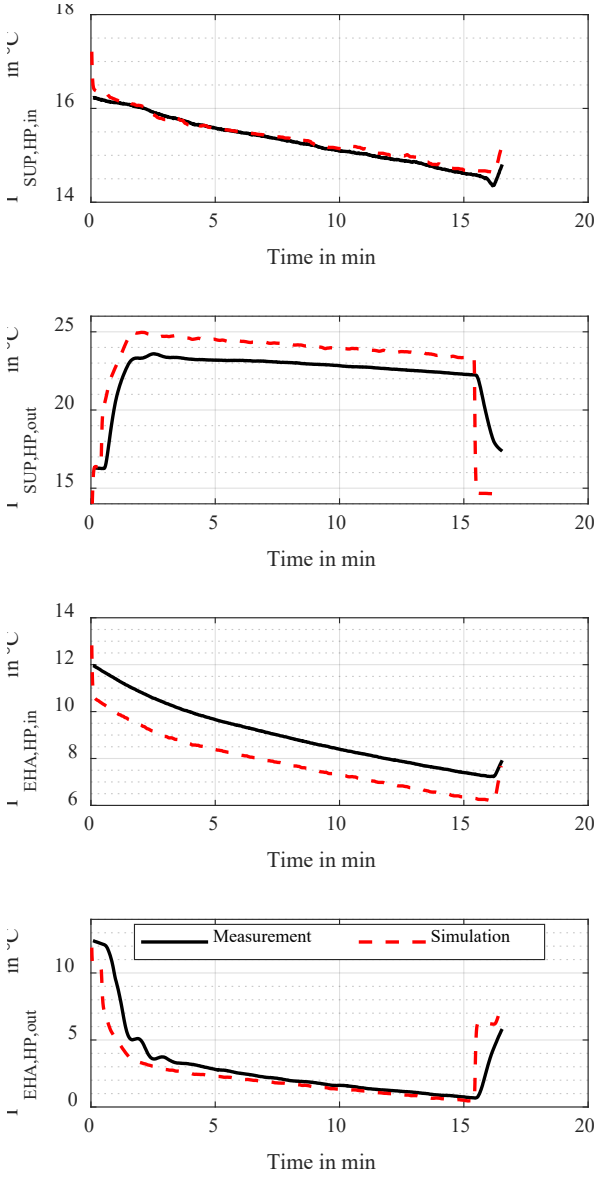

Fig. 11. Temperature comparison at heat pump in heating mode.

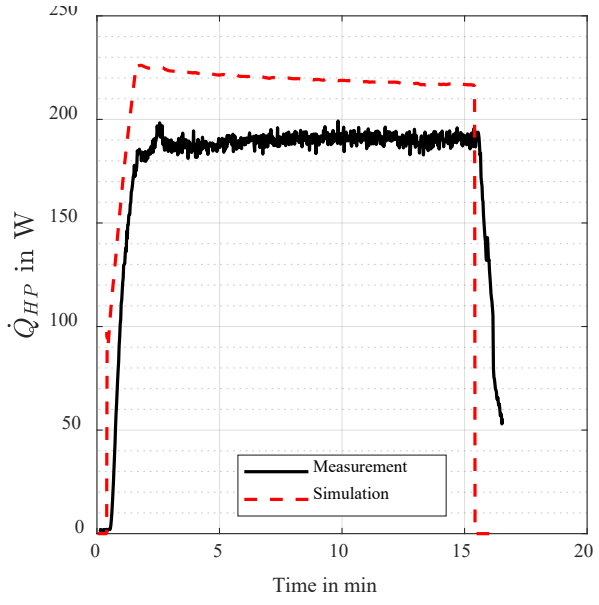

Fig. 12. Heat flow comparison at the condenser of the heat pump in heating mode.

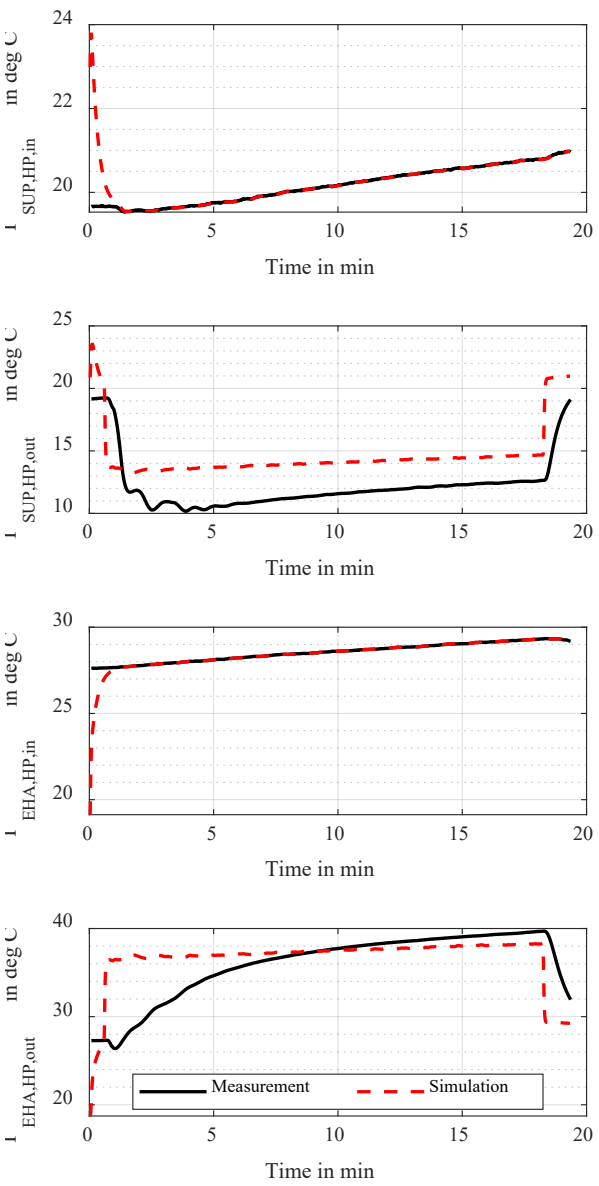

Fig. 13. Temperature comparison at heat pump in cooling mode.

Fig. 14. Heat flow comparison at the evaporator of the heat pump in cooling mode.

5 Conclusion

Renovation of buildings, especially the outer walls, will be an important factor for reducing CO_2 emissions in the building sector. Hence, mechanical ventilation units will be required after renovation. Decentral AHUs are one of multiple measures for integrating the mechanical ventilation units in buildings. If the decentral AHU include integrated heat pumps, it could be a fast-track measure since there is only an electrical socket required.

This paper presents a simulative design method, validated by a demonstrator. With a simulation model including the building, weather data and the AHU, it is possible to determine heating and cooling power demand for each component in stationary working points. These power demands are depending on the used efficiencies of the ERS and the heat pump, parameterized in the simulation model.

As a result, the topology with an EHA heat exchanger is preferable for the investigated type of building. In combination with the ERS, it has the lowest electrical energy demand of all investigated topologies, even if the heat pump is not operating with highest annual COP.

After building the demonstrator, stationary working points are compared in simulation and measurement. The ERS shows good validity since the heat flow differs with a maximum of 5 % to the simulation. The heat pump achieves a deviation of 13 % at heating and 25 % at cooling.

Finally, using simplified AixLib simulation models, components of a decentral AHU can be sized with simulation. Important is to define sufficient efficiencies in the models. In this paper a sensible efficiency of 75 % for the ERS and a carnot efficiency of 35 % of the heat pump is chosen.

6 Acknowledgement

Grateful acknowledgment is made for financial support by the Federal Ministry for Economic Affairs and Climate Action (BMWK), the ”DLR Projektträger” (DLR-PT) and the “Forschungsvereinigung für Luft- und Trocknungstechnik” (FLT) e.V., promotional reference IGF 21356 N/1.

Supported by:

Federal Ministry
for Economic Affairs
and Climate Action

on the basis of a decision
by the German Bundestag

References

1. W. Frenz, Das novellierte Klimaschutzgesetz, **Natur und Recht 43 Nr. 9**, 583 – 588 (2021)
2. J. Herkel, A. Burkhardt, R. Henger, B. Köhler, R. Meyer, S. Sommer, Y. Yilmaz, C. Kost, Maßnahmen und Instr. f. e. amb., klimafr. und sozialverträgliche Wärmewende im Gebäudesektor, **Teil 1** (2021)
3. BMWK, Energieeffizienzstrategie 2050 (2019)
4. M. Dunst, Lüftungsanlagen in öffentlichen Gebäuden, 17 – 20 (2022)
5. B. Bender, D. Göhlich, Dubbel Taschenbuch für Maschinenbau, **Bd. 25**, 871 – 954 (2018)
6. L. Maier, D. Jansen, F. Wüllhorst, M. Kremer, A. Kümpel, T. Blacha, D. Müller, AixLib: an open-source Modelica lib. for compound building en. sys. from comp. to district level with autom. quality management, Journal of building performance simulations (2023)
7. Schweizerischer Ingenieur- und Architekturverein (SIA), Raumnutzungsdaten für die Energie- und Gebäudetechnik, **SIA 2024** (2015)
8. Deutsche Norm, Energetische Bewertung von Gebäuden (DIN EN 16798-1), Teil 1: Eingangsparameter, (2021)
9. D. Jansen, J. Richarz, D. Vaeßen, D. Hering, D. Müller, Comparison of thermal simulation models with different levels of detail for non-residential buildings, in Proceedings of BauSim Conference 2022, 20-22 September, Weimar, Germany (2022)
10. A. Mardiana-Idayu, S. Riffat, An experimental study on the performane of ERS for buildling applications, in Journal of Energy and Buildings 43 (2011)
11. F. Possamai, M. Todescat, A Review of household compressor energy performance, in Proceedings of the International Compressor Engineering Conference, 12-15 July 2004, Purdue, USA (2004)
12. C. Vering, L. Maier, K. Breuer, H. Krützfeldt, R. Streblow, D. Müller, Eval. HP system design methods towards a sustainable heat supply in residential buildings, Journal of Applied Energy (2022)
13. Deutsche Norm, Ergonomie der thermischen Umgebung (DIN EN ISO 7730), (2006)
14. C. Höges, V. Venzik, C. Vering, D. Müller, Bewertung alternativer Arbeitsmittel für Wärmepumpen im Gebäudesektor, Forschungs im Ingenieurwesen, **Nr. 86**, 213 – 224 (2022)
15. W. Linck, M. Giebe, Bestimmung von Kältemittelfüllmenge und Sammlergröße für Kälteanlagen, DIE KÄLTE & Klimatechnik, **11/1999** (1999)
16. D. Calleja-Anta, L. Nebot-Andrés, j. Catalán-Gil, D. Sánchez, R. Cabello, R. Llopis, Thermodynamic screening of alternative refrigerants for R290 and R600a, in Journal of Results in Engineering (2020)